Investigation of the Influence of Varying Operation Configurations on Flow Behaviors Characteristics and Hydraulic Axial-Flow Pump Performance

Ahmed Ramadhan Al-Obaidi[1*], Hussam Ali Khalaf[2], Jassim Alhamid[3]

{ahmedram@uomustansiriyah.edu.iq}

[1]Department of Mechanical Engineering, College of Engineering, Mustansiriyah University, Baghdad, Iraq
[2]Department of Mechanical Engineering, College of Engineering, University of Thi-Qar, Iraq
[3]Washington State University, School of Mechanical and Materials Engineering, WSU Tri-Cities, USA

Abstract. To investigate the varying operating conditions characteristics in the axial flow pumps, The Computational Fluid Dynamics method is applied to achieve the unsteady flow simulation on flow pattern characteristics and hydraulic pump performance according to the turbulent model type of RNG k-ε turbulence. The reliability and accuracy of the CFD simulation results are compared and verified with a model test. Outcomes demonstrate that the flow field characteristics are changing with operating conditions change. The pressure variations are great near the tip blade, because of the effect of clearance backflow and high interactions flow in this region under the large flow condition. The results display that flow separation and tip leakage flow are accompanied by the high magnitude of the dynamic pressure value. The tip blade plays an important role at different flow rates due to the mixing and separation dominates. Hence, the tip blade deviation extremely influences the stable and safe operation of pump stations and axial pumps.

Keywords: Numerical analysis, Varying Operation Configurations, Flow Behaviours Characteristics, axial-flow pump impeller

1 Introduction

Axial-Flow Pumps are widely used in industrial and domestic applications which consume about 22% of the world's energy by electric motors [1–4] these types of Axial-Flow pumps had many problems like noise causes due to pump geometry complexity, vibration, cavitation phenomenon and flow conditions[5-6]. Zhang et al. [7] carried out a numerical study using CFD to investigate the performance of an Axial-Flow Pump. Their findings indicated that the pump could be utilized to represent flow patterns and energy consumption in a full-scale oxidation ditch. The impact of minimizing losses in the impeller's passage and outlet on the pump's performance was studied by [8] for various cases of passage width and outlet angle. Bashtani and Esfahani [9] conducted a numerical analysis of turbulent flow in double corrugated tubes. According to the findings, as the degree of corrugation increases, the Nusselt number increases in the same Reynolds number, with the Nusselt number of the corrugated pipe exceeding that of a simple smooth pipe by over 1.75 times and the effectiveness ratio by 1.73. In a distinct study by Al-Obaidi and Ali Ramadhyani [10-13],

ICONSEIR 2022, November 24, Medan, Indonesia

DOI 10.4108/eai.24-11-2022.2332719

which focused on heat transfer in corrugated flow channels at higher Reynolds numbers, it was observed that the Nusselt numbers surpassed those of a simple smooth pipe when the Reynolds number was over 1500. Stasiek et al. [14] reported that the friction factor rose by 130% to 280% while examining the effects of corrugated passages on the flow field and heat transfer. They discovered that the average Nusselt number increased with a rise in Reynolds number, while the friction coefficient reduced.

The study by Liu et al. [15] involved a numerical investigation of the internal flow in an axial flow pump, with a particular focus on the flow in spirally corrugated pipes and heat transfer on the shell side. Results of the study indicated an increase in heat transfer quantities ranging from 104 to 109.6% as well as an increase in pressure drops ranging from 1.21 to 1.08 times for corrugated tubes. The efficiency evaluation was found to be 1.35. Additionally, Fuqiang et al. [16] employed a Fluent CFD 3D model to predict the heat transfer characteristics and thermal deformation of corrugated pipes. The study demonstrated an 8.4% increase in the heat transfer coefficient and a reduction in thermal strain of the metal pipe by less than 13%. The results also indicated that flow separation and tip leakage flow were associated with a high magnitude of dynamic pressure and turbulent kinetic energy (TKE) values. The tip blade was found to play a significant role at various flow rates, primarily due to the prevalence of mixing and separation. Consequently, any deviation in the tip blade could significantly impact the safe and stable operation of pump stations and axial pumps.

2 Boundary Conditions and Computational Parameters

2.1 3D model

The axial-flow pump impeller's 3D model is shown in Figure 1, consisting of four blades, with speed of 3000 r/min and a flow rate of 12.5. The pump's flow passage has three sections: the stationary tapered inlet, the rotating impeller, and the stationary outlet. Figure 2 depicts the flow passage's division using unstructured grids, with a total of 910,000 grids. The incoming flow was assumed to be uniform, with the velocity of the inlet oriented perpendicular to the boundary surface of the inlet. The study employed non-slip boundary conditions in the near-wall area, with velocity input and pressure output. Gravity was also taken into account during the flow field calculation, with its direction reversed to match that the section opuf the mp outlet.

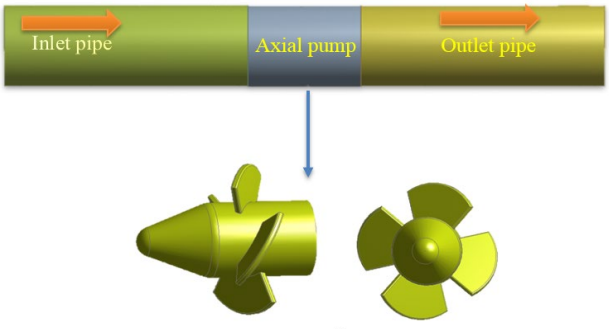

Fig. 1. Axial pump physical model

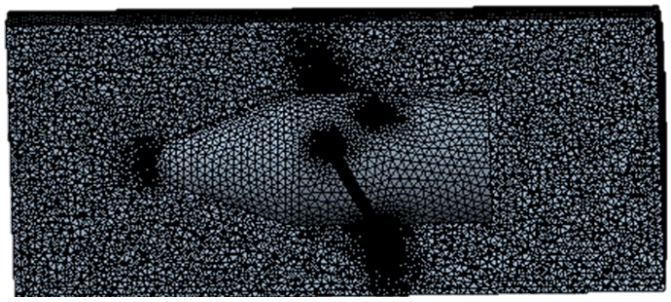

Fig. 2. Mesh of the Flow passage

2.2 Turbulence model

This paper utilized the nonlinear energy sink (NES) as the governing equation and employed a 3D Numerical model with the RNG k–ε turbulence [17-18]. The turbulence RNG k-ε model takes into account swirl flow and rotational conditions in the average flow by implementing a correction to the turbulent kinetic viscosity. The equations for k and ε in the RNG k-ε model are as follows:

$$\frac{\partial(\rho k)}{\partial(t)}+\frac{\partial(\rho k u_i)}{\partial(x_i)}=\frac{\partial}{\partial x_j}\left[\alpha_k \mu_{eff}\frac{\partial_k}{\partial x_j}\right]+\mu_t\left(\frac{\partial u_i}{\partial x_j}+\frac{\partial u_j}{\partial x_i}\right)\frac{\partial u_i}{\partial x_j}-\rho\varepsilon \quad (1)$$

$$\frac{\partial(\rho \varepsilon)}{\partial(t)}+\frac{\partial(\rho \varepsilon u_i)}{\partial(x_i)}=\frac{\partial}{\partial x_j}\left[\alpha_\varepsilon \mu_{eff}\frac{\partial_\varepsilon}{\partial x_j}\right]+\frac{C_{1\varepsilon}\varepsilon}{k}\mu_t\left(\frac{\partial u_i}{\partial x_j}+\frac{\partial u_j}{\partial x_i}\right)\frac{\partial u_i}{\partial x_j}-C_{2\varepsilon\rho}\frac{\varepsilon^2}{k} \quad (2)$$

Where x_j, x_i are the coordinate components, ρ is the density of the fluid, u_i, u_j are the time-averaged velocity components, μ_{eff} is the coefficient of effective turbulent flow viscosity μ_t is the turbulent viscosity, $\alpha_k \alpha_\varepsilon$ are the corresponding k and ε coefficients

$$\mu_{eff=\mu+\mu_t} \qquad \mu_t = \rho C_\mu \frac{k^2}{\varepsilon} \quad R = \frac{C_\mu \rho \emptyset^3 (1-\frac{\emptyset}{\emptyset_0}) e^2}{(1+\beta \emptyset^3) k}$$

Where C_μ= 0.00845, $C_{1\varepsilon}$= 1.42, $C_{2\varepsilon}$=1.68, $\emptyset = (2E_{ij})\frac{k}{\varepsilon}$

E_{ij} = ½$(\frac{\partial u_i}{\partial x_j}+\frac{\partial u_j}{\partial x_i})$, $\emptyset_0$=4.377, β=0.012

3 Results and Discussion

3.1 Numerical Model Validation

Under various flow conditions, the experimental and numerical hydrodynamic performance comparison [19] has been illustrated in Figure 3, compared with the RNG k- ε turbulence model, numerical outcomes by using SIMPLEC algorithm and couple pressure and velocity model are provided better agreement results as compared to the experimental data at

the different load boundary condition. Besides, the relative errors for both results maintain is lower than 7.5%. The SIMPLEC algorithm and RNG k-ε turbulence model with FLUENT CFD has been used, the pressure and the axial flow impeller velocity in the single-phase were solved.

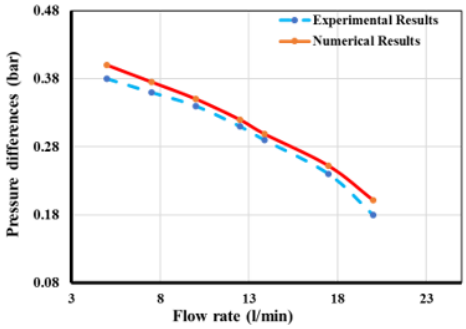

Fig. 3. Experimental and numerical data comparison

The flow patterns in the blades of the axial pump were analyzed in Figure 5, showing that the presence of a solid phase results in increased axial velocity in the radial direction between the flange to the hub and a corresponding decrease in liquid phase velocity. The velocity of water along the pump blades surface shows a progressive rise in relative velocity from the hub to the flange in the radial direction when the water is clear, thus supporting the cylindrical layer assumption were independence. The axial velocity behind the blade experiences a decrease in the flow direction. In the working area, the velocity reduces between the inlet to the outlet, followed by a subsequent increase towards the outlet. Additionally, the velocity relative to the working face is lower than that of the back.

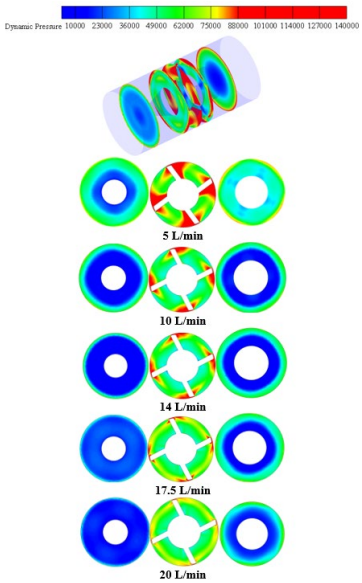

Fig. 4. Under different conditions dynamic pressure variations

The distribution of axial velocity of a liquid on the blades of an axial flow pump. shown in Figure 5, reveals that the velocity can increase radially from the hub to the flange due to the existence of a solid phase, which causes a decrease in the liquid's velocity. The velocity distribution in the vicinity of the axial flow pump blade surface in clear water shows a progressive rise in the relative velocity along the radial direction, from the hub to the flange. This observation provides evidence to support the hypothesis that the cylindrical layer operates autonomously. In the flow direction, the axial velocity at the rear of the blade reduces gradually. Also, at the working face, the axial velocity declines from the inlet towards the outlet, but rises again before reaching the outlet. Additionally, the relative velocity at the working face is lower compared to that of the back.

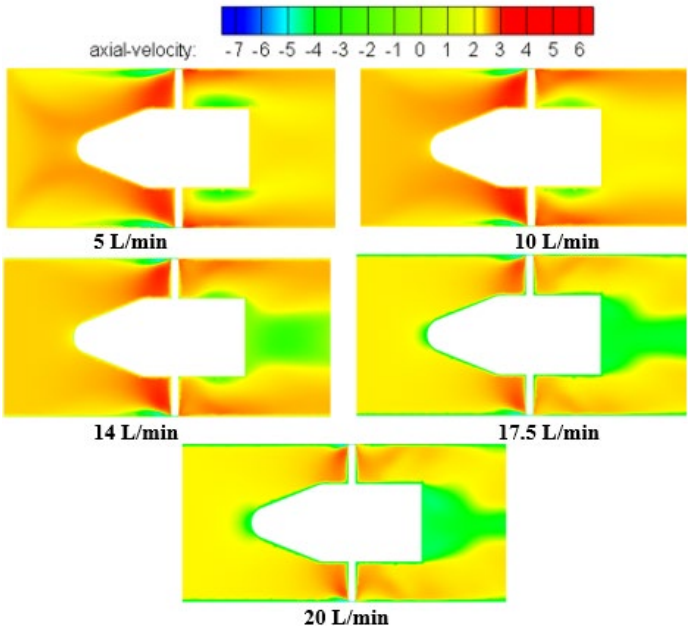

Fig. 5. Under different conditions axial velocity variations

3.2 Analysis of Pressure Fluctuations in the Impeller Blade

In the next section, Fluent CFD is used to analyze the pressure fluctuations in impeller blades under various operating conditions, based on the aforementioned findings. Pressure fluctuations are an unavoidable phenomenon in pumps and can significantly affect inside the pump the transient flow field analysis. Therefore, studying the characteristics of pressure fluctuations can offer valuable insights into the pump's behavior, such as the impeller's impact on the pipe wall during different operating conditions. Figure 6 illustrates the pressure oscillations occurring in the impeller blades under different operating conditions, such as using a four-blade impeller, rotating at around 3000 rpm, and with a circumference of 102 mm. The flow rates tested were 5, 7.5, 10, 12.5, 17.5, and 20 (l/min). For point 1 in the figure, there are four peaks and four valleys observed under different flow rates. For each flow rate,

the average pressure at monitoring point 1 is depicted, revealing a noticeable reduction in the average pressure as the flow rate rises.

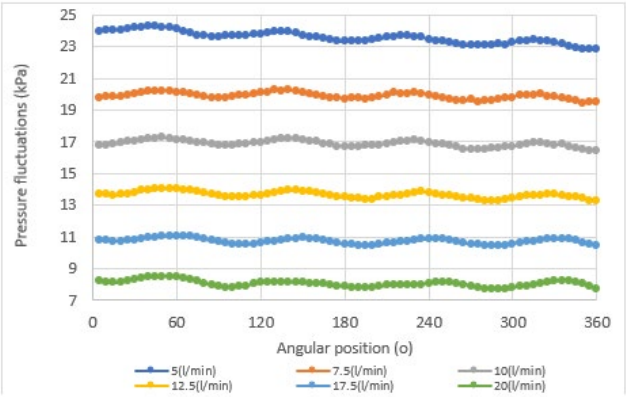

Fig. 6. Pressure Fluctuations at Monitoring Point 1 Across Various Flow Rates

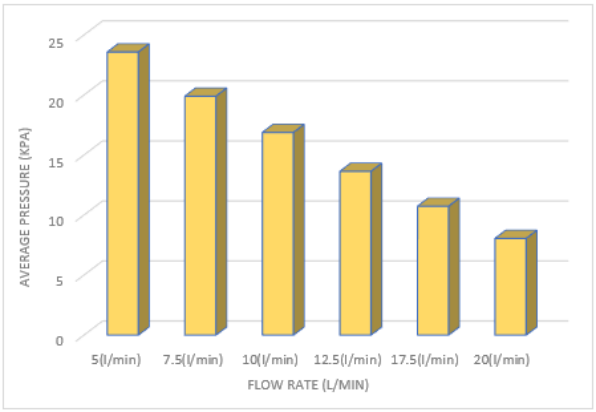

Fig. 7. Variation of Average Pressure at Monitoring Point 1 with Flow Rates

4 Conclusions

The results obtained from numerical simulations indicate various effects of different flow conditions on the turbulent flow produced by the axial flow pump under investigation. Firstly, Pump pressure increases from the impeller outlet to the pump inlet region, with the greatest pressure measured at the impeller outlet region. Secondly, the pressure on the suction surface of the impeller blades is lower than that at the outlet due to the influence of pressure distribution. Thirdly, when the flow rate is around 5 liters per minute, the high-speed region is detected close to the blade and blade tip area on the middle surface. Axial impellers have a low-pressure zone at their outlet when flow is increased. In addition, the numerical simulation demonstrated both positive and negative pressure in certain areas of the blade. This phenomenon can lead to cavitation due to a decrease in water pressure below the water vapor pressure within those regions.

Acknowledgements

The author would like to thank Mustansiriyah University (www.uomustansiriyah.edu.iq) Baghdad – Iraq for its support in the present work.

References

[1] Wang, C., Shi, W., Wang, X., Jiang, X., Yang, Y., Li, W., & Zhou, L. (2017). Optimal design of multistage centrifugal pump based on the combined energy loss model and computational fluid dynamics. Applied Energy, 187, 10-26.

[3] Al-Obaidi, A. R. (2021). Numerical investigation on effect of various pump rotational speeds on performance of centrifugal pump based on CFD analysis technique. International Journal of Modeling, Simulation, and Scientific Computing, 2150045.

[4] Al-Obaidi, A. R. (2020). Experimental investigation of cavitation characteristics within a centrifugal pump based on acoustic analysis technique. International Journal of Fluid Mechanics Research, 47(6).

[5] Olszewski, P., & Arafeh, J. (2018). Parametric analysis of pumping station with parallel-configured centrifugal pumps towards self-learning applications. Applied energy, 231, 1146-1158.

[6] Al-Obaidi, A. R., & Alhamid, J. (2021). Numerical investigation of fluid flow, characteristics of thermal performance and enhancement of heat transfer of corrugated pipes with various configurations. In Journal of Physics: Conference Series (Vol. 1733, No. 1, p. 012004). IOP Publishing.

[7] Zhang, Y., Zheng, Y., Fernandez-Rodriguez, E., Yang, C., Zhu, Y., Liu, H., & Jiang, H. (2016). Optimization design of submerged propeller in oxidation ditch by computational fluid dynamics and comparison with experiments. Water Science and Technology, 74(3), 681-690.

[8] Shojaeefard, M. H., Tahani, M., Ehghaghi, M. B., Fallahian, M. A., & Beglari, M. (2012). Numerical study of the effects of some geometric characteristics of a centrifugal pump impeller that pumps a viscous fluid. Computers & Fluids, 60, 61-70.

[9] Bashtani, I., & Esfahani, J. A. (2019). ε-NTU analysis of turbulent flow in a corrugated double pipe heat exchanger: A numerical investigation. Applied Thermal Engineering, 159, 113886.

[10] Ali, M. M., & Ramadhyani, S. (1992). Experiments on convective heat transfer in corrugated channels. EXperimental Heat Transfer an International Journal, 5(3), 175-193.

[11] Al-Obaidi, A. R. (2021). Analysis of the Effect of Various Impeller Blade Angles on Characteristic of the Axial Pump with Pressure Fluctuations Based on Time-and Frequency-Domain Investigations. Iranian Journal of Science and Technology, Transactions of Mechanical Engineering, 45(2), 441-459.

[12] Al-Obaidi, A. R. (2020). Influence of guide vanes on the flow fields and performance of axial pump under unsteady flow conditions: Numerical study. Journal of Mechanical Engineering and Sciences, 14(2), 6570-6593.

[13] Al-Obaidi, A. R. (2020). Experimental comparative investigations to evaluate cavitation conditions within a centrifugal pump based on vibration and acoustic analyses techniques. Archives of Acoustics, 45(3), 541-556.

[14] Stasiek, J., Collins, M. W., Ciofalo, M., & Chew, P. E. (1996). Investigation of flow and heat transfer in corrugated passages—I. Experimental results. International Journal of Heat and Mass Transfer, 39(1), 149-164.

[15] Liu, J. J., Liu, Z. C., & Liu, W. (2015). 3D numerical study on shell side heat transfer and flow characteristics of rod-baffle heat exchangers with spirally corrugated tubes. International Journal of Thermal Sciences, 89, 34-42.

[16] Fuqiang, W., Qingzhi, L., Huaizhi, H., & Jianyu, T. (2016). Parabolic trough receiver with corrugated tube for improving heat transfer and thermal deformation characteristics. Applied energy, 164, 411-424.
[17] Li, Y. J., & Wang, F. J. (2007). Numerical investigation of performance of an axial-flow pump with inducer. Journal of hydrodynamics, 19(6), 705-711.
[18] Al-Obaidi, A. R. (2021). Investigation of the flow, pressure drop characteristics, and augmentation of heat performance in a 3D flow pipe based on different inserts of twisted tape configurations. Heat Transfer.
[19] Mostafa, N. H., & Mohamed, A. (2012). Effect of blade angle on cavitation phenomenon in axial pump. J Appl Mech Eng, 1(112), 2.